



INEEL/CON-03-01183  
PREPRINT

## CHF Enhancement By Vessel Coating For External Reactor Vessel Cooling

J. Yang  
M. B. Dizon  
F. B. Cheung  
J. L. Rempe  
K. Y. Suh  
S. B. Kim

June 13-17, 2004

ICAPP '04

*This is a preprint of a paper intended for publication in a journal or proceedings. Since changes may be made before publication, this preprint should not be cited or reproduced without permission of the author. This document was prepared as an account of work sponsored by an agency of the United States Government. Neither the United States Government nor any agency thereof, or any of their employees, makes any warranty, expressed or implied, or assumes any legal liability or responsibility for any third party's use, or the results of such use, of any information, apparatus, product or process disclosed in this report, or represents that its use by such third party would not infringe privately owned rights. The views expressed in this paper are not necessarily those of the U.S. Government or the sponsoring agency.*

## CHF Enhancement by Vessel Coating for External Reactor Vessel Cooling

**J. Yang, M. B. Dizon, and F. B. Cheung**

*Department of Mechanical & Nuclear Engineering  
Pennsylvania State University, University Park, PA 16802, USA  
fxc4@psu.edu*

**J. L. Rempe**

*Idaho National Engineering and Environmental Laboratory  
P.O. Box 1625, Idaho Falls, ID*

**K. Y. Suh**

*Department of Nuclear Engineering, Seoul National University  
Seoul, Korea*

**S. B. Kim**

*Korea Atomic Energy Research Institute, P.O. Box 105, Yuseoung  
Taejon, Korea*

**Abstract** –*In-vessel retention (IVR) is a key severe accident management (SAM) strategy that has been adopted by some operating nuclear power plants and advanced light water reactors (ALWRs). One viable means for IVR is the method of external reactor vessel cooling (ERVC) by flooding of the reactor cavity during a severe accident. As part of a joint Korean – United States International Nuclear Energy Research Initiative (K-INERI), an experimental study has been conducted to investigate the viability of using an appropriate vessel coating to enhance the critical heat flux (CHF) limits during ERVC. Toward this end, transient quenching and steady-state boiling experiments were performed in the SBLB (Subscale Boundary Layer Boiling) facility at Penn State using test vessels with micro-porous aluminum coatings. Local boiling curves and CHF limits were obtained in these experiments. When compared to the corresponding data without coatings, substantial enhancement in the local CHF limits for the case with surface coatings was observed. Results of the steady state boiling experiments showed that micro-porous aluminum coatings were very durable. Even after many cycles of steady state boiling, the vessel coatings remained rather intact, with no apparent changes in color or structure. Moreover, the heat transfer performance of the coatings was found to be highly desirable with an appreciable CHF enhancement in all locations on the vessel outer surface but with very little effect of aging.*

### I. INTRODUCTION

In-vessel retention (IVR) is a key severe accident management strategy<sup>1</sup> that has been adopted by some operating nuclear power plants and some advanced light water reactors (ALWRs) such as the Korean Advanced Power Reactor APR1400 and the Westinghouse's Advanced Plants AP600 and AP1000. One viable means for IVR is the method of external reactor vessel cooling (ERVC) of the reactor pressure vessel (RPV) by flooding of the reactor cavity during a severe accident. With water

covering the lower external surfaces of the RPV, significant energy (i.e., decay heat) could be removed from the core melt through the vessel wall by downward-facing boiling on the vessel outer surface. As long as the choking limit for steam venting (CLSV) is not exceeded and the wall heat flux from the core melt is lower than the critical heat flux (CHF) limit for boiling on the vessel outer surface, nucleate boiling would be the prevailing regime.<sup>2</sup> In that case, the vessel outer surface temperature could be maintained near the saturation temperature of water such

that the reactor vessel could be sufficiently cooled to maintain the RPV integrity.

In spite of its importance, only few researchers have investigated the subject of ERVC. The only relevant studies available in the literature are those by Chu et al.,<sup>3</sup> Theofanous et al.,<sup>4</sup> Rouge et al.,<sup>5</sup> Cheung et al.,<sup>6</sup> and Chang and Jeong.<sup>7</sup> Chu et al. used the CYBL facility for a full-scale simulation of the downward facing boiling process on the outer surface of a reactor lower head.<sup>3</sup> Two types of steady-state boiling experiments were performed. The first applied a uniform heat flux to the vessel whereas the second delivered a higher heat flux near the edge. For all the experiments performed, the bottom center was found to have the highest temperature even when the edge heat flux was higher than that at the bottom center. Visual observations were made that clearly revealed the cyclic nature of the vapor dynamics for the downward facing boiling process and the resulting two-phase motion along the heating surface. However, the CHF phenomenon was not observed in their experiments.

Theofanous et al. conducted a full scale simulation of the downward facing boiling process on the outer surface of a hemispherical reactor vessel using a two-dimensional copper slice with independently heated zones in the ULPU facility at UCSB.<sup>4</sup> Five configurations were employed in their experiments, aiming at providing a foundation to allow implementation of the IVR concept to Westinghouse's Advanced LWR designs. Configurations I, II and III were primarily for AP600 whereas Configurations IV and V were for AP1000. Configuration I simulated the process of downward facing boiling on the external bottom center of the vessel, covering the region of  $-30^\circ < \theta < 30^\circ$  where  $\theta$  was measured from the stagnation point. Configuration II simulated a full side of a reactor lower head from the bottom center all the way up to the equator ( $0^\circ < \theta < 90^\circ$ ). Configuration III was similar to configuration II with the addition of a panel to simulate the thermal insulation structure. Their data revealed a significant spatial variation of the critical heat flux with the angular position,  $\theta$ , of the vessel. However, the insulation structure (Configuration III) was found to have very little effect on the local CHF limit.

In an attempt to explore the effect of the flow path on the CHF limits, Theofanous et al. performed 28 burnout experiments using Configuration IV that incorporated a baffle into the ULPU-2000 facility to simulate an alternate geometry of the reflecting insulation around the RPV.<sup>4c</sup> The baffle served to streamline the flow path between the RPV surface and the insulation. Results of the ULPU-IV experiments showed that streamlining the flow path around the lower head was beneficial to CHF performance under IVR conditions. However, at the very top of the heated wall ( $90^\circ$ ), a sudden drop in the local CHF was observed.

They attributed this decrease in CHF to the exit phenomena that affected the local flow structure. To address and overcome the exit phenomena found in ULPU-IV tests, four major modifications were made in Configuration V in the ULPU-2400 facility.<sup>4d</sup> These modifications included the inlet baffle and baffle entry, an adjustable baffle around the vessel lower head, a smooth transition from the baffle to the riser, and a nozzle that simulated transition from the riser to the inclined duct. Thirty-six burnout tests were conducted in three series. It was found that the local CHF limits in the heater's uppermost region could exceed  $1.8 \text{ MW/m}^2$ , with the local CHF limit at  $90^\circ$  approaching a value of  $\sim 2.0 \text{ MW/m}^2$ .

Rouge investigated the coolability of a large-scale structure by water under natural convection conditions in the SULTAN facility.<sup>5</sup> He measured the main characteristics of a two-dimensional two-phase flow and evaluated the natural circulation mass flow behavior in a large system. He reported that for an optimized flow path, a heat flux higher than  $1.0 \text{ MW/m}^2$  could be removed from the wall by natural circulation. He concluded that it was possible to maintain large-scale vessel coolability under natural convection conditions. Later, Rouge et al. carried out additional campaigns, with each of them exploring one particular inclination angle and gap size, in the SULTAN facility.<sup>5b</sup> For a given cover pressure, inlet subcooling and uniform heat flux, they gradually reduced the mass velocity until the limit of boiling crisis was detected. In addition to the CHF limits, they also observed the two-phase flow in the SULTAN channel. Dry patches were found to be rather small (on the order of 2 to 6  $\text{cm}^2$ ) and would not expand much. Most of the dry patches occurred near the end of the heated section but some were also present at lower elevations. An empirical CHF correlation was developed from the data, in terms of the cover pressure, mass velocity, local quality, gap size, and inclination angle. Their experimental results indicated favorable possibilities for long-term coolability of corium under natural convection conditions.

Cheung et al. studied the downward facing boiling and critical heat flux phenomena on the outer surface of a hemispherical vessel using the SBLB (Subscale Boundary Layer Boiling) test facility at PSU.<sup>6</sup> The facility provides a three-dimensional simulation of the downward facing boiling process on the outer surface of a hemispherical reactor vessel with and without a surrounding insulation structure. The test section of the facility was designed such that it can be readily interchanged to simulate various boiling and flow configurations. To establish a baseline case for comparison, Cheung et al. employed the SBLB facility to study the downward facing boiling process and CHF phenomenon on the external surface of a reactor vessel simulator without an insulation structure.<sup>6a</sup> A significant spatial variation of the critical heat flux, with

the local CHF limit increasing monotonically from the bottom center to the equator of the vessel, was measured for both saturated and subcooled boiling.

Having established the baseline case, Cheung et al. employed the SBLB facility to study the downward facing boiling process and CHF phenomenon on the external surface of a reactor vessel simulator with a surrounding insulation structure.<sup>6b,6c</sup> The latter included both the AP600 and KNGR insulation configurations. In both cases, an internal upward co-current two-phase flow was observed in the annular channel between the insulation structure and the test vessel. At the same heat flux level, more flow was induced along the vessel outer surface for the case with insulation compared to the case without. As a result, the nucleate boiling heat transfer and the critical heat flux for the case with insulation were found to be consistently higher than those for the corresponding case without insulation. In addition to the magnitude of the critical heat flux, the insulation structure also affected the spatial variation of the CHF limit. For the case with insulation, the local critical heat flux no longer increased monotonically in the flow direction. Rather, it decreased from the bottom center toward the downstream locations, exhibiting a minimum near the minimum gap of the annular channel, before it increased toward the equator of the vessel. Some noted differences in the steam venting process through the minimum gap region and the local CHF variations along the vessel outer surface, were observed between the AP600 and KNGR systems.

Recently, Cheung et al.<sup>6d,6e</sup> and Dizon et al.<sup>8</sup> investigated the downward facing boiling process and CHF phenomenon on the external surface of a reactor vessel surrounded by a scaled APR1400 insulation structure in the SBLB facility, aimed at developing methods for ERVC enhancement during IVR under severe accident conditions. Two distinctly different methods were investigated to enhance external cooling of the APR1400 reactor vessel. One involved the use of an enhanced vessel/insulation design to facilitate steam venting through the bottleneck of the annular channel between the RPV and its surrounding insulation structure. The other involved the use of an appropriate vessel coating to promote the downward facing boiling process on the vessel outer surface. Both methods were found to lead to considerable increase in the local CHF limits.

Chang and Jeong performed a preliminary study in the KAIST facility to measure the CHF values at different mass flux levels using a 2-D slice test section to simulate the APR1400 vessel configuration.<sup>7a</sup> Under the same mass flux conditions, the CHF values obtained in their facility were found to be consistently lower than those of the ULPU data. They attributed the differences to a smaller gap size used in the KAIST facility. When compared their

CHF data with the SULTAN correlation, they found that the latter overestimated the KAIST data. Later, Jeong et al., measured the CHF values for different mass flux levels and various degrees of inlet subcooling under forced circulation conditions.<sup>7b</sup> They found that the CHF values were consistently lower than those of the ULPU data, similar to the results reported by Chang and Jeong.<sup>7a</sup> They attributed the differences to a smaller gap size and different test section material and thickness used in the KAIST facility. They also attributed the differences to different flow circulation conditions (i.e., natural circulation in the ULPU facility as compared to forced circulation in the KAIST facility). In addition to ULPU data, they also compared their CHF data with the values predicted by SULTAN correlation. They found that for high mass fluxes ( $\sim 150 \text{ kg/m}^2\text{s}$ ), the SULTAN correlation compared favorably with their measured data. However, under low mass flux conditions, the SULTAN correlation failed to predict their CHF data. Using the hydrodynamic CHF model developed by Cheung and Haddad<sup>9</sup> for downward facing curved surfaces, effect of the mass flux on the CHF was identified, from which Jeong et al.<sup>7b</sup> were able to correlate their CHF data satisfactorily with the mass flux for a given inlet subcooling.

Although ERVC appears to be a viable means for IVR, it is not clear that ERVC without additional enhancements could provide sufficient cooling for high-power reactors such as APR1400. To improve the margin for IVR in high-power reactors, a three-year project entitled, "In-Vessel Retention Strategy for High Power Reactors," funded by the joint United States/Korean International Nuclear Energy Research Initiative (I-NERI) program, was launched to develop recommendations to improve the margin for IVR in high power reactors. Transient quenching and steady-state boiling experiments were performed under simulated ERVC conditions in the SBLB facility using test vessels with micro-porous aluminum coating. This paper reports the local boiling curves and CHF limits obtained in these ERVC simulation experiments.

## II. SBLB EXPERIMENTS

Transient quenching and steady state boiling experiments were conducted in the SBLB facility to investigate the separate effects of vessel coating on CHF enhancement. Test vessels with and without coatings were employed in these tests. The experimental apparatus, measurement techniques, and experimental procedure are described below.

### II.A. Experimental Apparatus

The SBLB test facility consisted of a water tank with a condenser assembly (see Fig. 1), a heated hemispherical

test vessel with or without an insulation simulator, a data acquisition system, a photographic system, and a power control system. The water tank had a diameter of 1.22 m and a height of 1.14 m. One small and two large windows were placed on two opposite sides of the tank. One large window was used for the recording system along with light sources and the other was used for additional lighting as deemed necessary. The small window was used to observe the water level while the tank was being filled with water. The windows were fastened to the tank by placing a ring on the outside of the window that was bolted to a flange. An O-ring seal was used to prevent any leaks around the windows. The tank was equipped with three immersion heaters with a total power of 36 kW for preheating the water in the tank. A condenser assembly was installed on top of the tank to maintain the water level and the pressure of the tank constant during an experiment.

The test vessel was comprised of two main parts made of aluminum: a heated lower hemispherical vessel and a non-heated upper cylindrical portion. The upper cylindrical portion had an outside diameter of 0.3 m and a wall thickness of 12.7 mm. The lower end of the upper portion had a 25.4 mm flange with a 6.35-mm groove for an o-ring and twelve 4.7 mm screw holes for attaching the upper portion to the lower hemispherical vessel. The latter had a bottom-heated section and an upper heated section. The bottom heated section consisted of inner and outer segments that were welded together and heated independently. The weld that kept the two segments together was placed on the outside at the interface between the two segments and it was the main region of contact between the two sections. Everywhere else along the circumference that separated the inner and outer segments, there was 3.18 mm air gap to minimize conduction heat transfer between the two segments. A 3.18 mm groove was also placed along the outer circumference of the outer segment to minimize heat conduction to the rest of the test vessel. The upper heated section consisted of three independently heated segments. A 0.00475-m groove was cut between segments to reduce heat conduction between them.

Cartridge heaters, 31.75 mm long and 9.52 mm thick, were employed to provide independent heating of the five segments. For the proper operations of these heaters, it was very important to minimize the air gap between the heaters and the test section. Therefore, the holes for the heaters were drilled and then reamed to provide a 0.0254 mm fit. Before inserting them in the holes, the heaters were treated with a special coating called Watlube from Watlow. This product protected against high temperature oxidation and more importantly it enhanced the heat transfer between the heaters and the test section. There were up to 32 K-type thermocouples installed in the vessel to monitor and record the temperature of the wall.



Figure 1. An Overall View of the SBLB Water Tank with an APR1400 Vessel/Insulation Simulator

### *II.B. Measurement Techniques*

The temperature at various locations of the vessel was monitored by using a 25 MHz 386 IBM compatible personal computer along with a data acquisition system. Two Strawberry Tree CPC-16 boards were installed inside the PC. Each of these boards had 16 analog inputs and 16 digital input/output channels. The CPC-16 board was capable of resolutions in the range between 12 and 16 bits, which was equivalent to 0.024% and 0.0015% of full scale, respectively. Each of the boards had six voltage ranges that could be set according to the sensor used. The boards also had a high noise rejection integration converter, which helped reject 50/60 Hz AC power line interference when used in the "low noise mode". The CPC-16 units were also capable of accurate cold junction compensation and linearization for thermocouple devices. The two ACPC-16 boards were connected to a total of four Strawberry Tree T12 boards, which in turn were connected to the thermocouples. Each of the T12 boards had 8 analog inputs and 8 digital input/output channels. Based on the procedure

outlined by Haddad<sup>10</sup> and Liu<sup>11</sup>, the uncertainty in the temperature measurements was estimated to be  $\pm 0.38$  °C. For heat flux levels above  $0.1 \text{ MW/m}^2$ , the temperature measurements were estimated to be  $\pm 7\%$ . Some selected experiments were repeated to confirm the reproducibility of the data.

The Quicklog program, developed by Strawberry Tree, was used to both monitor and record the vessel wall temperatures during the heating and quenching process, respectively. The sampling rate was set at 20 Hz, with a resolution of 0.006% (14 bits), and was operated at Fast Mode (maximum board speed). For steady state experiments, the speed of the data collection was not that critical. The data acquisition program was also used to create a control routine that used to protect the vessel from any possible meltdown in the high heat flux regime. When the critical heat flux was reached during steady state boiling experiments, any further increase in the power input would result in the onset of film boiling. This was characterized by an abrupt increase in the local temperature of the heating surface. In order to protect the vessel against any possible meltdown, a power control mechanism was installed to discontinue the power supply to the heaters when a significant jump in the vessel temperature was detected in the high heat flux regime. The power control system consisted of a data acquisition system, a constant DC power source, a solid-state relay, and thermocouples to measure the vessel wall temperatures. The solid-state relay had a low voltage side connected to the constant DC power source, and a high voltage side connected to the variac supplying the heaters. The solid-state relay was needed because the high voltage of the variac could not be connected directly to the digital I/O channel of the data acquisition board.

To carry out the control strategy, a control routine was created using the computer program Quicklog from Strawberry Tree Inc. This routine started by collecting the temperatures of the vessel wall at several desired locations. These temperatures were then compared to a set point value of  $250^\circ\text{C}$ , which was much higher than the expected wall temperature that was characteristic of nucleate boiling in water. Wall temperatures higher than  $250^\circ\text{C}$  could have only been due to the occurrence of the critical heat flux. Under normal operating conditions, the vessel wall temperature would be less than  $250^\circ\text{C}$  and the digital I/O channel connected to the solid-state relay would be closed. This allowed the high voltage side of the solid-state relay to stay closed for the desired power to be delivered to the vessel. When a wall temperature greater than  $250^\circ\text{C}$  was detected, the digital I/O channel became open. As a result, the low voltage side of the solid-state relay was not powered anymore and the power supply to the heaters was discontinued, which prevented any further substantial increase in the vessel wall temperature.

### *II.C. Experimental Procedure*

To prepare for a run, the tank was filled with water to the desired level. A pump was used to circulate the water through a high-performance filter. This helped remove the particles that precipitated during the heating process. Then the immersion heaters were turned on to heat the water to a prescribed temperature. If the temperature fell below the desired value during an experiment, one of the heaters was turned on again to bring the water temperature back up. Before every experiment, the water was given time to become completely quiescent. In these tests, saturation temperature was maintained for the water in the tank.

Transient quenching experiments were conducted under atmospheric conditions (101 kPa) and at saturation temperature ( $100^\circ\text{C}$ , no subcooling) using hemispherical aluminum vessels to investigate the spatial variation of the boiling curve and CHF limit along the vessel outer surface. Several 203.2 mm diameter aluminum hemispherical shells (3.175 mm thick) were ordered and were then machined. A 6.35 mm thick aluminum annular flange was welded onto the rim of the hemisphere to allow for mounting to a cover fixture. Eight holes were drilled and tapped on the flange to allow the assembled hemisphere to mate with a stainless steel cover assembly that mounted to the control rod, i.e., the test-module sliding mechanism. This connector allowed the hemispherical assembly to be screwed onto the control rod. The rod was used to lower and raise the hemispherical vessel during quenching. Thermocouple wires were also run through the inside of the rod. A high temperature gasket was then installed between the welded flanged and cover fixture to ensure a leak tight fit.

To record the local temperature-time histories during quenching (and hence derive the local boiling curves) at different angular positions, K-type thermocouples (Glass Braided, 30 AWG) were installed inside the hemispherical vessel. The thermocouples were inserted in drilled holes, with a depth of around 1.5 mm, to improve the accuracy of the measured temperature. The thermocouple holes or pits where drilled on the inside surface along an arc in the angular direction,  $\theta$ . The first hole was centered at the bottom of the hemisphere,  $\theta = 0^\circ$ . Subsequent holes were then drilled with a circumferential spacing of 12.5 mm. A total of 12 thermocouple holes were drilled, each having a depth of about 1.5 mm. Three additional, equally spaced thermocouples were also mounted inside the hemisphere to monitor the temperature at various locations and ensure uniform heating. Thermocouples were attached to the hemisphere using either Omega's OB-200 epoxy or CC High Temp cement.

Steady state boiling experiments were also conducted to obtain the nucleate boiling portion of the boiling curve. In these experiments, the water was conditioned and heated

to the prescribed temperature. The power supply cables and the thermocouple wires were then connected to the adjustable power suppliers and the data acquisition system, respectively. Each power supply circuit was equipped with a multimeter that allowed the voltage across and current through the adjustable power suppliers to be measured. Next, the power sources to the adjustable power suppliers were turned on and the variac and/or SCR were set to deliver the desired heat flux level. At the same time, the temperatures at various locations inside the vessel wall were monitored on the computer screen using the data acquisition program Quicklog from Strawberry Tree Inc. Once it was decided that steady state conditions were reached, the program Quicklog was used to record the steady state temperatures at various locations of the vessel wall and store them into a file for analysis.

Whenever it was decided to video tape the boiling process, a high speed Ektapro video camera system by Kodak was turned on after the desired steady state conditions had been reached. Then, the lighting was adjusted until a satisfactory image of the flow was obtained. The boiling process was also photographed directly using a digital camera and was then stored on the computer. Two types of steady state boiling tests were conducted, one using plain test vessels whereas the other using coated vessels. By comparing the results obtained in these two types of tests, the separate effect of vessel coating could be determined.

### III. RESULTS AND DISCUSSION

#### III.A. Boiling Data for Plain Vessels

The nucleate boiling curves for a plain vessel without coatings at different heat flux levels measured at various locations of the test vessel under saturated boiling conditions are shown in Figs. 2 to 6. In these figures, the local boiling heat fluxes are plotted against the local wall superheats with the angular position as a parameter. In each graph, the local boiling curve obtained by the transient quenching technique and the corresponding local nucleate boiling curve obtained by the steady state boiling experiments are presented for comparison. As can be seen from these figures, for all locations on the vessel outer surface, the steady state boiling data were consistently higher than those determined from the transient quenching experiments, particularly at moderate high flux levels. These results are similar to those reported by Haddad for a plain vessel obtained under identical test conditions.<sup>10</sup>

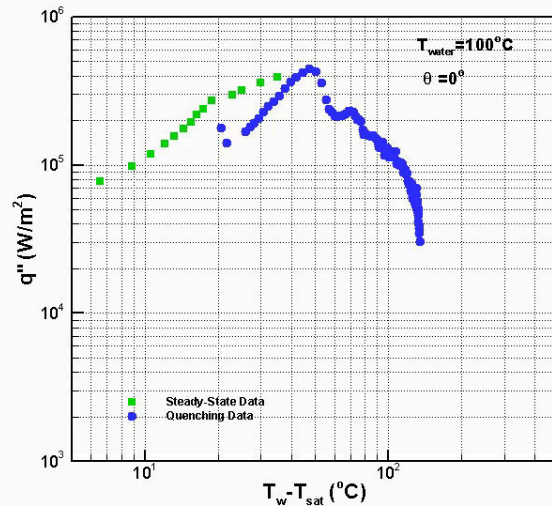


Figure 2. Local Boiling Curve at the Bottom Center (0°) of a Plain Vessel

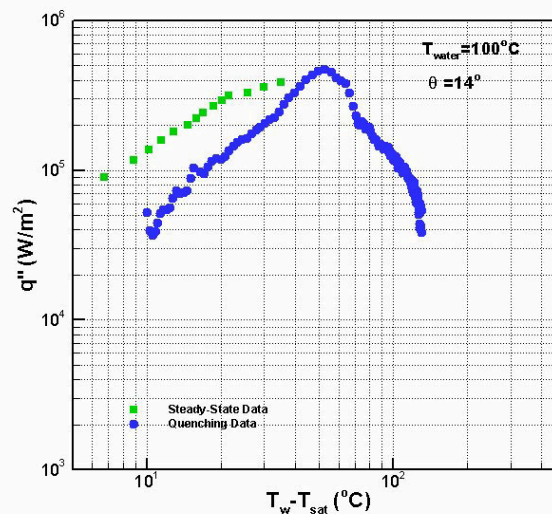


Figure 3. Local Boiling Curve at an Off-Center Location (14°) of a Plain Vessel

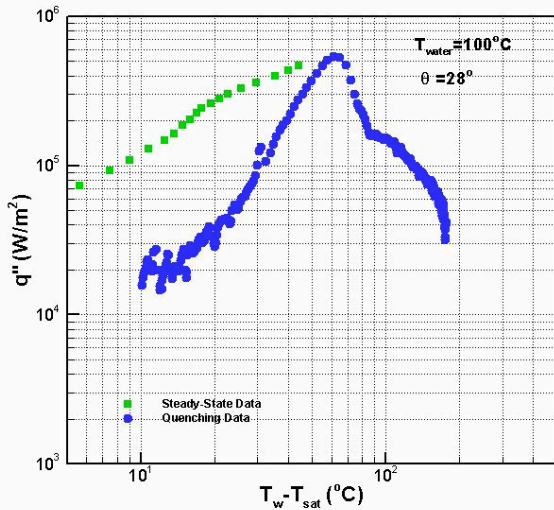


Figure 4. Local Boiling Curve at an Off-Center Location (28°) of a Plain Vessel

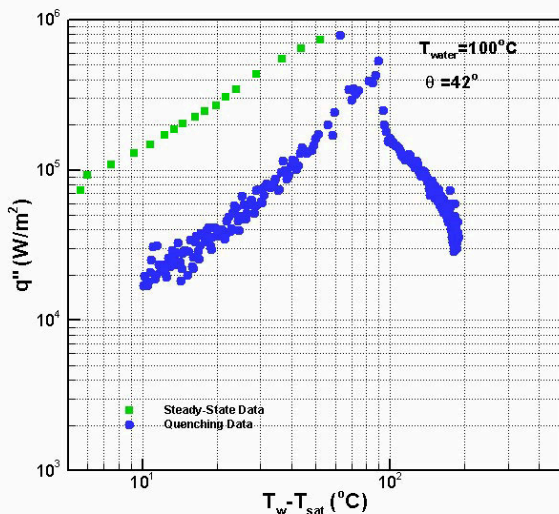


Figure 5. Local Boiling Curve at an Off-Center Location (42°) of a Plain Vessel

A possible explanation for the above results is that there were errors associated with the data deduced from the transient experiments in the final stage of quenching. An order-of-magnitude analysis of the quenching process indicated that the time scales for the initial and intermediate stages of quenching were sufficiently large for the flow to establish a quasi-steady behavior. However, the time scale for the final stage of quenching, corresponding to the nucleate boiling regime, was much too small for adequate flow development. As a result, the quenching data underestimated the nucleate boiling rate because of the transient effect. Nevertheless, the difference between the steady state and transient data became smaller as the

heat flux level was increased. The local CHF limits obtained in the steady state experiments appeared to be very close to those deduced from the transient quenching data.

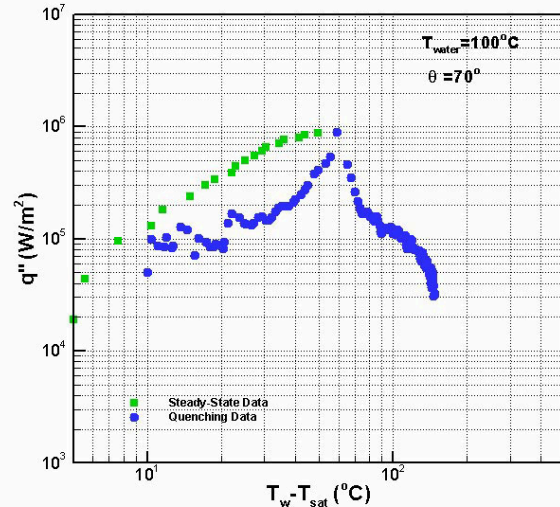


Figure 6. Local Boiling Curve at an Off-Center Location (70°) of a Plain Vessel

By comparison of the steady state boiling data obtained at various angular positions shown in Figs. 2 to 6, it can be seen that in the nucleate boiling regime, the local boiling curve tended to shift upward and to the right as the angular position was increased from the bottom center toward the equator of the test vessel. For a given wall superheat, higher nucleate boiling rates were obtained in the locations downstream of the bottom center. The local CHF increased monotonically with the angular position from the bottom center to the equator of the vessel. These results are quite similar to those reported by Haddad<sup>10</sup> for a plain vessel.

### III.B. Boiling Data for Vessels with Micro-Porous Aluminum Coating

Transient quenching and steady state boiling experiments were performed in the SBLB facility using test vessels with micro-porous aluminum coatings. The local boiling curves at different heat flux levels measured at various locations of the test vessel under saturated boiling conditions are shown in Figs. 7 to 11. In these figures, the local boiling curves obtained by the transient quenching technique and the corresponding local nucleate boiling curves obtained by the steady state boiling experiments are presented in the same graphs for comparison. For all locations on the vessel outer surface, the steady state boiling data were consistently higher than those determined from transient quenching experiments,



particularly at moderate high flux levels. These results are similar to those observed for a plain vessel.

Owing to the transient effect mentioned in the preceding section, the quenching data underestimated the nucleate boiling rate. Nevertheless, the difference between the steady state and transient data became smaller as the heat flux level was increased. The local CHF limits obtained in the steady state experiments appeared to be very close to those deduced from the transient quenching data. Unlike the trend observed for plain vessels, the local boiling curve for coated vessels did not shift monotonically upward and to the right as the angular position was increased from the bottom center toward the equator of the test vessel. Rather, the local CHF appeared to exhibit a local minimum at the  $\theta = 14^\circ$  location. This non-monotonic behavior was not observed for a plain vessel.

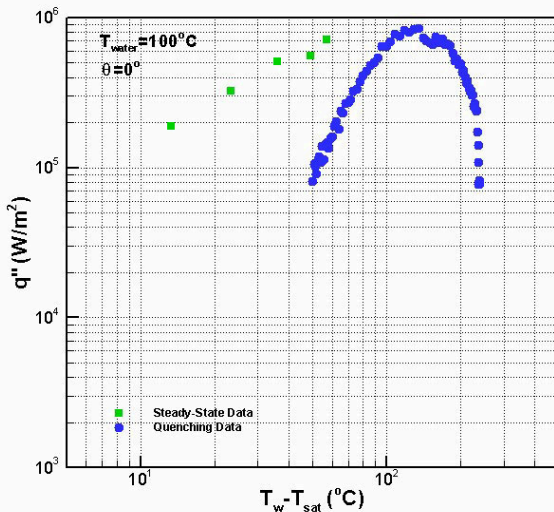


Figure 7. Local Boiling Curve at the Bottom Center ( $0^\circ$ ) of a Coated Vessel

It should be mentioned that the micro-porous aluminum coatings appeared to be very durable. Even after many cycles of steady state boiling, the vessel coatings remained rather intact, with no apparent changes in color or structure. Nevertheless, newly coated vessels were used to repeat some selected steady state boiling tests. The results were well within the uncertainties of the experimental measurements. The effect of aging was found to be of secondary importance.

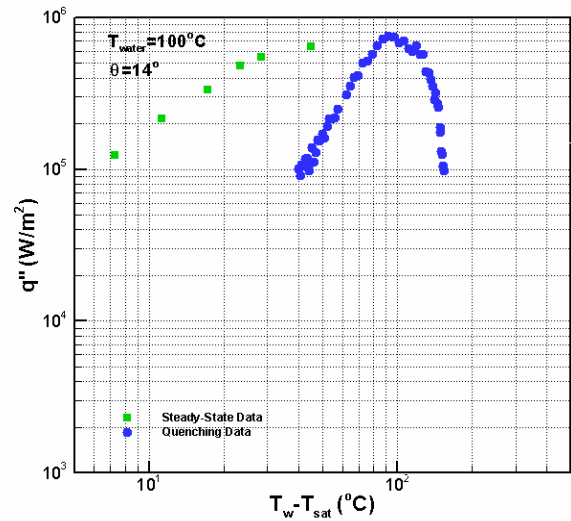


Figure 8. Local Boiling Curve at an Off-Center Location ( $14^\circ$ ) of a Coated Vessel

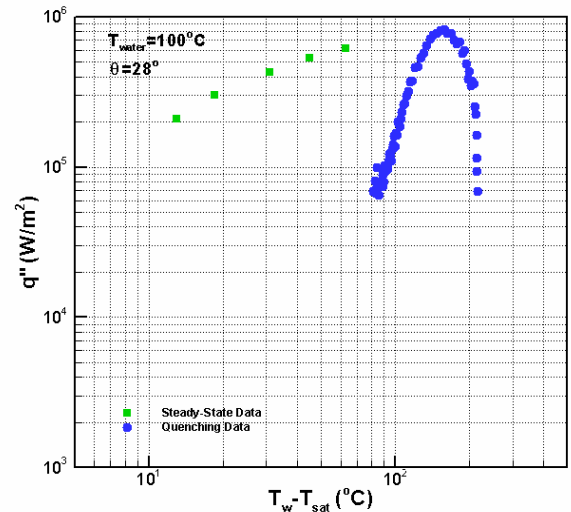


Figure 9. Local Boiling Curve at an Off-Center Location ( $28^\circ$ ) of a Coated Vessel

### III.C. Effect of Vessel Coatings on the Local CHF Limits

To quantitatively determine the effect of vessel coatings, the local boiling curve at a given angular position obtained for micro-porous aluminum coating is compared to the corresponding boiling curve for a plain vessel, as shown in Figs. 12 to 16. In each figure, the boiling curves for the plain and coated vessels were constructed using the results presented in Figs. 2 to 11. The steady state boiling data were employed in constructing the nucleate boiling portion of the curve whereas the transient quenching data were employed in constructing the remaining portion of the

boiling curve. This approach was deemed appropriate, as the steady state boiling data were more reliable and accurate than the transient quenching data in the nucleate boiling regime. The boiling curves shown in these figures provided a more realistic representation of the actual boiling behavior on the vessel outer surface.

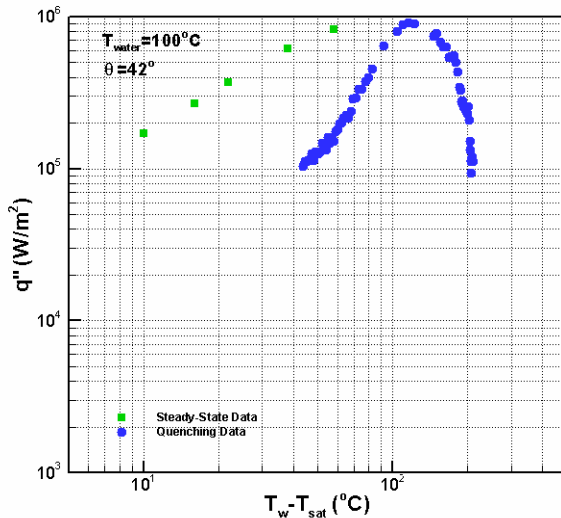


Figure 10. Local Boiling Curve at an Off-Center Location (42°) of a Coated Vessel

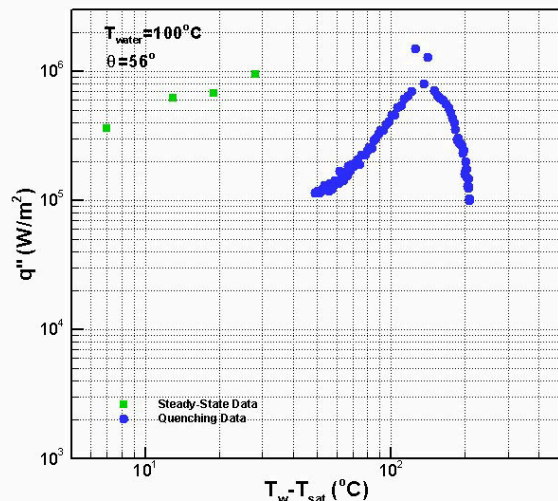


Figure 11. Local Boiling Curve at an Off-Center Location (56°) of a Coated Vessel

As can be seen from Figs. 12 to 16, for all angular positions, the local boiling curves for the coated vessel were consistently higher than those corresponding boiling curves for a plain vessel. The local boiling curve for a coated vessel tended to shift upward and to the right relative to the corresponding local boiling curve for a plain vessel. Hence a higher local CHF limit could be achieved

by using micro-porous aluminum coatings. In addition to the magnitude of the local CHF limit, the corresponding wall superheat at which CHF occurred was also higher for the coated vessel. It should be noted that the effect of coating was not uniform over the entire vessel outer surface. The extent of CHF enhancement and the increase in the corresponding wall superheat depended on the particular angular position.

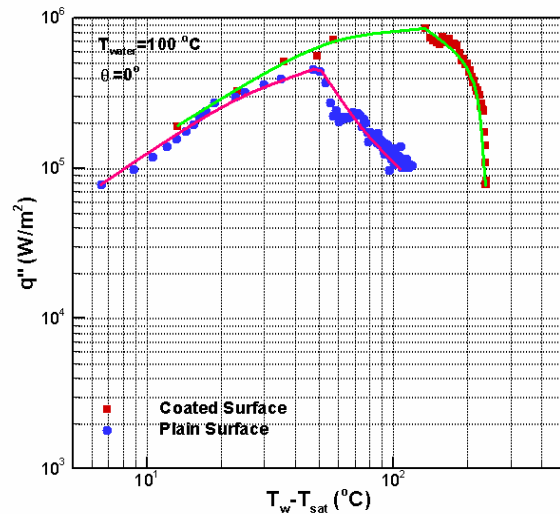


Figure 12. Comparison of the Local Boiling Curves at the Bottom Center (0°)

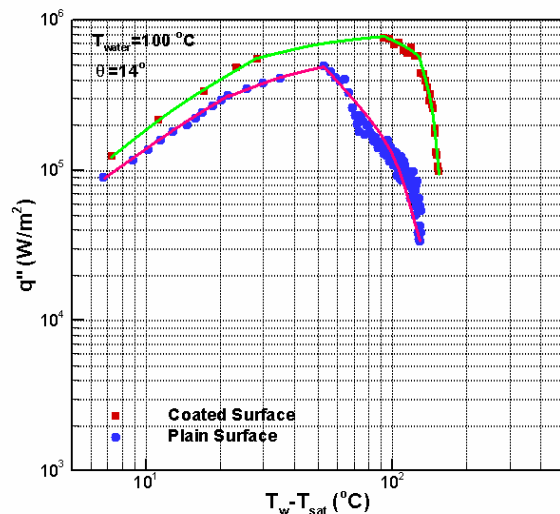


Figure 13. Comparison of the Local Boiling Curves at an Off-Center Location (14°)

It should be noted from the above figures that for vessels with surface coatings, the local CHF limit at the bottom center,  $\theta = 0^\circ$ , was higher compared to the local CHF values at the  $\theta = 14^\circ$  or  $28^\circ$  locations. The higher CHF at the bottom center was believed to be attributed to

the divergence effect of the  $\theta = 0^\circ$  location. For coated vessels, the bottom center could be thought of as a singularity point, where there was liquid supply from all radial directions. During steady state boiling of water on the outer surface of a coated vessel, the micro-porous layer

were less liquid supply routes in the other angular locations. As a result, the local CHF limits at the  $\theta = 14^\circ$  and  $28^\circ$  locations were smaller than that at the bottom center.

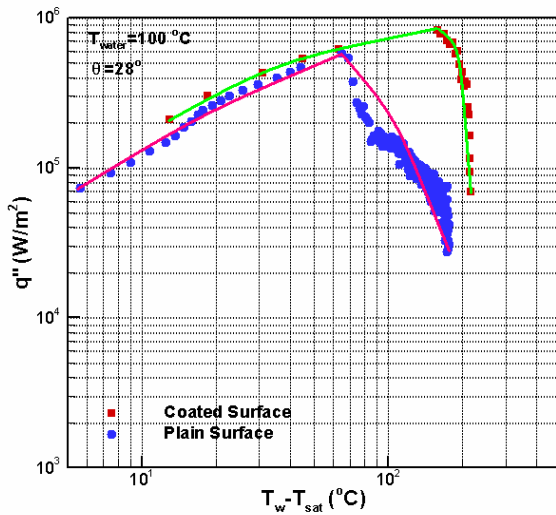


Figure 14. Comparison of the Local Boiling Curves at an Off-Center Location (28°)

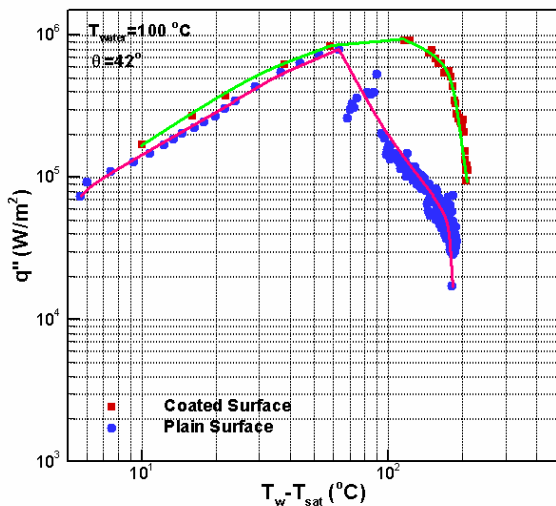


Figure 15. Comparison of the Local Boiling Curves at an Off-Center Location (42°)

allowed liquid to be supplied from all directions within the porous coating structure. This helped prevent local dryout at the bottom center, thereby increasing the local CHF limit. On the other hand, for other angular locations away from the bottom center, liquid supply was possible only through a longitudinal direction, i.e. from above and below, since in the latitudinal direction, there was minimum liquid supply due to symmetry. Thus, unlike the bottom center, there

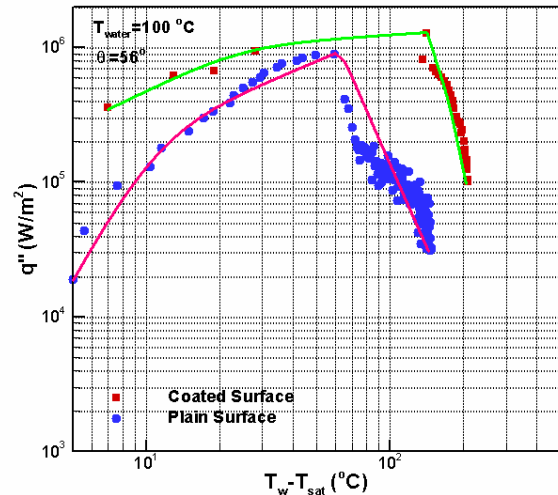


Figure 16. Comparison of the Local Boiling Curves at an Off-Center Location (56°)

At locations further downstream, however, the two-phase flow effect and the influence of the local orientation became more pronounced. The local CHF limit increased toward the equator of the test vessel with values well above the local CHF limit at the bottom center.

#### IV. CONCLUSIONS

Based on the results of the transient quenching and steady state boiling experiments obtained in the SBLB test facility, the following conclusions can be made:

1. The steady state boiling data were consistently higher than those determined from transient quenching experiments, particularly at moderate high flux levels. This trend was observed for both the plain and coated vessels. The quenching data underestimated the nucleate boiling rate because of the transient effect. Nevertheless, the difference between the steady state and transient data became smaller as the heat flux level was increased. The local CHF limits obtained in the steady state experiments were very close to those deduced from the transient quenching data.
2. By combining the steady state boiling and transient quenching data, more meaningful boiling curves could be constructed for the plain and coated vessels. At a given angular position, the steady state boiling data were employed in constructing the nucleate boiling portion of the curve whereas the transient quenching data were employed in constructing the

remaining portion. This approach provided a more realistic representation of the boiling curves, as the steady state boiling data were more reliable and accurate than the transient quenching data in the nucleate boiling regime.

3. For plain vessels without coatings, the local boiling curve tended to shift upward and to the right as the angular position was increased from the bottom center toward the equator of the test vessel. For a given wall superheat, higher nucleate boiling rates were obtained in the locations downstream of the bottom center. The local CHF exhibited a minimum at the bottom center location and increased monotonically with the angular position toward the equator of the vessel.
4. Compared to a plain vessel, the micro-porous coated vessel consistently increased the local CHF values for all angular locations. Unlike the trend observed for plain vessels, the local boiling curve for coated vessels did not shift monotonically upward and to the right as the angular position was increased from the bottom center toward the equator of the test vessel. The local CHF limit at the bottom center was actually higher than the values for adjacent downstream locations up to  $\theta = 28^\circ$ . The local CHF exhibited a minimum at the  $\theta = 14^\circ$  location rather than at the bottom center. This non-monotonic behavior of the local CHF variation was largely due to the capillary effect of the micro-porous coatings, where there was continuous liquid supply from all radial directions toward the bottom center.
5. Micro-porous aluminum coating appeared to be very durable. Even after many cycles of steady state boiling, the vessel coating remained rather intact, with no apparent changes in color or structure. Moreover, the heat transfer performance of the coating was found to be highly desirable with an appreciable CHF enhancement but very little effect of aging.

#### ACKNOWLEDGMENTS

This work was performed under DOE contract number DE-AC07-99ID13727. The authors are grateful for the financial support by the U.S. Department of Energy and the Korean Ministry of Science and Technology as part of the K-INERI program.

#### REFERENCES

1. Rempe, J. L., Suh, K. Y., Cheung, F. B., and Kim, S. B., In-Vessel Retention Strategy for High Power

Reactors, *2002 Annual Report*, INEEL/EXT-02-01291, (2002).

2. Cheung, F. B., "Limiting Factors for External Reactor Vessel Cooling," *Keynote Lecture KL-09*, NURETH-10, (2003).
- 3a. Chu, T. Y. et al., "Observation of the Boiling Process from a Large Downward Facing Torispherical Surface," *Proceedings National Heat Transfer Conference*, (1995).
- 3b. Chu, T. Y. et al., "Ex-vessel boiling Experiments: Laboratory and Reactor-Scale Testing of the Flooded Cavity Concept for In-Vessel Core Retention," *Nuclear Engineering and Design*, Vol. 169, pp. 77-88, (1997).
- 4a. Theofanous, T. G. et al., "In-Vessel Coolability and Retention of a Core Melt," *DOE/ID-10460*, Advanced Reactor Severe Accident Program, Department of Energy, (1996).
- 4b. Theofanous, T. G. and Syri, S., "The Coolability Limits of a Reactor Pressure Vessel Lower Head," *Nuclear Engineering and Design*, Vol. 169, pp. 59-76, (1997).
- 4c. Theofanous, T. G. et al., "The Boiling Crisis Phenomenon - Part 1. Nucleation and Nucleate Boiling Heat Transfer; Part 2 - Dryout Dynamics and Burnout," *J. Experimental Thermal and Fluid Science*, Vol. 26, pp. 775-810, (2002).
- 4d. Theofanous, T. G. et al., "Limits of Coolability in the AP1000-Related ULPU-2400 Configuration V Facility," Paper G00407, NURETH-10, (2003).
- 5a. Rouge, S., "SULTAN Test Facility for Large-Scale Vessel Coolability in Natural Convection at Low Pressure," *Nuclear Engineering and Design*, Vol. 169, pp. 185-195, (1997).
- 5b. Rouge, S., Dor, I. and Geffraye, G., "Reactor Vessel External Cooling for Corium Retention SULTAN Experimental Program and Modeling with CATHARE Code," *Workshop Proceedings on In-Vessel Core Debris Retention and Coolability*, NEA/CSNI/R (98) 18, Garching, Germany, (1999).
- 6a. Cheung, F.B., Haddad, K. and Liu, Y.C., "Critical Heat Flux (CHF) Phenomena on a Downward Facing Curved Surface," *NUREG/CR-6507*, U.S. Nuclear Regulatory Commission, Washington, D.C., (1997).

- 6b. Cheung, F. B. and Liu, Y. C., "Critical Heat Flux (CHF) Phenomenon on a Downward Facing Curved Surface: Effects of Thermal Insulation," *NUREG/CR-5534*, U.S. Nuclear Regulatory Commission, Washington, D.C., (1998).
- 6c. Cheung, F. B. and Liu, Y. C., "Critical Heat Flux Experiments to Support In-Vessel Retention Feasibility Study for an Evolutionary Advanced Light Water Reactor Design," EPRI Technical Report-1003101, (2001).
- 6d. Cheung, F. B., Yang, J., Dizon, M. B., Rempe, J. L., Suh, K. H. and Kim, S. B., "Scaling of Downward Facing Boiling and Steam Venting in a Reactor Vessel/Insulation System," *Proceedings 2003 ASME Summer Heat Transfer Conference*, Paper HT2003-47208, (2003).
- 6e. Cheung, F. B., Yang, J., Dizon, M. B., Rempe, J. L., Suh, K. H. and Kim, S. B., "On the Enhancement of External Reactor Vessel Cooling of High-Power Reactors," Paper G00403, NURETH-10, (2003).
- 7a. Chang, S. H. and Jeong, Y. H., "CHF Experiments for External Vessel Cooling Using 2-D Slice Test Section," *SAMSON Seminar on In-Vessel Retention Strategy for High-Power Reactors*, Seoul National University, (2002).
- 7b. Jeong, Y. H., Chang, S. H. and Baek, W. P., "CHF Experiments on the Reactor Vessel Wall Using 2-D Slice Test Section," Paper G00314, NURETH-10, (2003).
8. Dizon, M. B., Yang, J., Cheung, F. B., Rempe, J. L., Suh, K. H. and Kim, S. B., "Effects of Surface Coating on Nucleate Boiling Heat Transfer on a Downward Facing Surface," *Proceedings 2003 ASME Summer Heat Transfer Conference*, Paper HT2003-47209, (2003).
9. Cheung, F.B. and Haddad, K., "A Hydrodynamic Critical Heat Flux Model for Saturated Pool Boiling on a Downward Facing Curved Heating Surface," *International Journal of Heat and Mass Transfer*, Vol. 40, No. 6, pp. 1291-1302, (1997).
10. Haddad, K. H., "An Experimental and Theoretical Study of Two-Phase Boundary Layer Flow on the Outside of Curved Downward-Facing Surfaces," Ph.D. Dissertation, Pennsylvania State University, University Park, (1996).
11. Liu, Y. C., "Buoyancy-Driven Co-Current Two-Phase Flow in a Hemispherical Annular Channel with Natural Convection Boiling on the Downward Facing Side," Ph.D. Dissertation, Pennsylvania State University, University Park, (1999).